Frequency doubling with $KNbO_3$ in an external cavity

E. S. Polzik and H. J. Kimble

Norman Bridge Laboratory of Physics, 12-33, California Institute of Technology, Pasadena, California 91125

Received May 14, 1991

Potassium niobate is employed in an external resonator to generate single-frequency tunable radiation near 430 nm. For excitation with 1.35 W of power from a cw titanium–sapphire laser, 0.65 W of blue light is produced. A simple model has been developed to account for thermal lensing in the nonlinear crystal.

Owing to the large second-order susceptibility of potassium niobate ($KNbO_3$), nonlinear mixing in $KNbO_3$ has been found to be an attractive source of blue light.[1–7] For example, a cw power of 40 mW at 429 nm has been achieved by frequency doubling of a semiconductor diode laser,[6] while 150 mW of power at 467 nm has been generated by nonlinear mixing of diode and Nd:YAG lasers in $KNbO_3$.[7] Although much of the research in this area has employed external buildup cavities to enhance the conversion efficiency, the absolute blue power has been limited by the available pump power. In this regard, the titanium–sapphire ($Ti:Al_2O_3$) laser is a suitable source since single-frequency output power in excess of 2 W is readily achieved. Indeed, the $Ti:Al_2O_3$ laser has recently been used for external-cavity doubling with $LiIO_3$ to produce 40 mW of broadly tunable blue output light for 600 mW of infrared input.[8] For doubling schemes with $KNbO_3$ within the $Ti:Al_2O_3$ laser cavity, 100–150 mW of blue light power near 430 nm has been obtained in unpublished experiments in our laboratory and elsewhere.[3]

Motivated by these developments as well as by a variety of possible applications in optical physics, we have undertaken an investigation of frequency doubling with $KNbO_3$ in an external buildup cavity driven by the light from a cw $Ti:Al_2O_3$ laser. We have made measurements of conversion efficiency over a range of operating conditions and have compared these results in absolute terms with those of a simple theoretical model. In a cw mode of operation, 0.65 W of blue light near 430 nm has been generated for 1.35 W of fundamental input. Because thermal lensing significantly affects the conversion efficiency and cavity servo performance at these power levels, we have also employed a transient mode of operation with the cavity length swept through resonance to obtain peak power of 1.0 W of blue light for 2.0 W of infrared excitation.

For our experiment, a single-frequency $Ti:Al_2O_3$ laser capable of producing as much as 2 W of output near 840–870 nm and with a linewidth of 50 kHz rms was mode matched into a ring doubling cavity resonant with the fundamental input (Fig. 1). The doubling cavity consisted of four flat mirrors and two lenses (f = 35 mm) together with a normal-cut $KNbO_3$ crystal of length 6 mm (Ref. 9); the crystal as well as lens surfaces were antireflection coated for low loss at both 860 and 430 nm. In spite of the quality of coatings (0.15%/surface), passive losses from the lenses reduced the cavity buildup relative to astigmatically compensated cavities with curved mirrors. However, the setup shown in Fig. 1 facilitates the exploration of a range of focusing geometries, which is of special importance since it allows fine tuning of the cavity mode to compensate for effects of thermal lensing at high power.

As for the theoretical expectation for the harmonic output, we recall the treatment by Ashkin *et al.*[10] for second-harmonic generation in an external resonator. If we denote the overall conversion efficiency by $\epsilon \equiv P_2/P_1$, with P_1 the fundamental input power and P_2 the harmonic output power, then a simple calculation yields

$$\sqrt{\epsilon} = \frac{4T_1\sqrt{E_{NL}P_1}}{[2 - \sqrt{1 - T_1}(2 - L - \sqrt{\epsilon E_{NL}P_1})]^2}, \quad (1)$$

where E_{NL} is the single-pass nonlinear conversion efficiency in the absence of the resonator ($E_{NL} = P_2/P_1^2$ for $T_1 = 1$), T_1 is the transmission coefficient of the input coupler, and L describes all linear losses in the cavity exclusive of T_1 (L and T_1 both refer to the fundamental field; the harmonic field is not resonant in the cavity). Equation (1) leads to an optimum value T_1^0 for maximum efficiency ϵ^0,

$$T_1^0 = L/2 + \sqrt{L^2/4 + E_{NL}P_1}. \quad (2)$$

It is straightforward to show that T_1^0 corresponds to an impedance-matched cavity[11] with zero reflection for the fundamental field. For our experiments all relevant parameters of the external doubling cavity C2 were directly measured. E_{NL} was measured by replacing the input coupler of the mode-matched cavity with a transparent window, with the result that $E_{NL} = 0.005\ W^{-1}$. Note that for optimum focusing external to the cavity and free from its constraints, we found that $E_{NL} = 0.016\ W^{-1}$, which is 30% lower than the best value that has been reported. Linear losses $L = (4.0 \pm 0.5)\%$ were calculated directly from the finesse of the cavity observed with the input coupler replaced by a high reflector. For these parameters, T_1^0 then ranged from 4% to 10% depending on the input power.

From the measured values for E_{NL} and L and with $T_1 = T_1^0$, the theoretical result for the optimum

0146-9592/91/181400-03$5.00/0

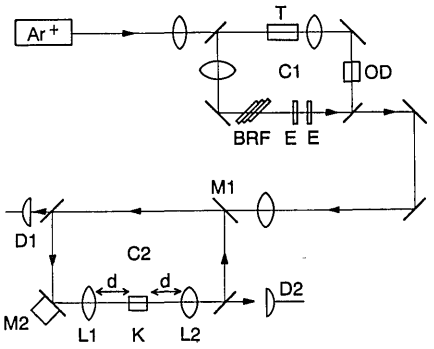

Fig. 1. Diagram of the principal components, with C1 the cavity of the Ti:Al_2O_3 laser and C2 the external doubling cavity with the $KNbO_3$ crystal. Elements of C1: BRF, birefringent filter; E's, étalons; OD, optical diode; T, laser crystal. Elements of C2: M1, input coupler; M2, piezoelectric-mounted mirror; L1, L2, lenses; K, $KNbO_3$ crystal. Detector D1 is for $\lambda_1 \simeq 860$ nm, while detector D2 is for $\lambda_2 \simeq 430$ nm.

harmonic output $P_2 = \epsilon^0 P_1$ is shown in Fig. 2 as a function of P_1. Also plotted in the figure are our experimental results for P_2 versus P_1 obtained for cw operation as well as for a swept mode of operation. For cw operation, the external cavity was locked to an incident fundamental resonance with a FM sideband technique.[12] In the swept mode, the cavity length was scanned so that the dwell time on resonance was sufficiently fast (~1 ms) to avoid thermal effects in the crystal. In either cw or swept mode, the temperature of the $KNbO_3$ crystal and the spacing d between the lenses and the crystal (Fig. 1) were slowly varied to maximize the harmonic output power P_2. Each experimental point is likewise taken for T_1 close to the optimum T_1^0 for the particular P_1. From Fig. 2 we see that up to an input power $P_1 = 1.0$ W and second-harmonic output power $P_2 = 0.5$ W the experimental results for cw operation agree reasonably well with theory. However, for higher powers, there is significantly less cw blue power than the simple theory predicts. To investigate this point further, we also show results obtained for a swept regime of operation in which thermal effects are greatly diminished and in which the agreement between experiment and the theory of Eq. (1) is quite satisfactory. The maximum peak power of blue that we have obtained in the swept regime is $P_2 = 1$ W at 430 nm for $P_1 = 2$ W at 860 nm. In terms of tunability, we have explored a range from 427 to 438 nm and found $\epsilon \simeq 0.5$ for $P_1 = 1$ W in the cw mode independent of λ.

Clearly then the thermal effects associated with the difference between our results for cw and swept observation warrant study in more detail. First, as for the source of heating, note that thermal gradients in the $KNbO_3$ crystal are produced by absorption from both fundamental and harmonic beams. Although the absorption at the fundamental is small (~0.5%), the circulating power is 10–15 W, so that the power deposited in the crystal (~60 mW) is comparable with that from the harmonic beam, whose absorption around 430 nm is ~8%. The importance of the combined heating from the fundamental and harmonic beams is demonstrated by the fact that the oven temperature for optimum phase matching in the cw regime is 1–3°C lower than for swept operation with $P_1 = 0.5$–1.4 W (recall that the single-pass phase-matching width for a 6-mm length of $KNbO_3$ is 0.5°C).

With regard to the effects of the heating on the system's performance, note that the absorbed light power drives a radially varying temperature distribution $T(r)$ within the crystal, which in turn gives rise to a spatially dependent index of refraction $n(r)$. The thermal lens associated with $n(r)$ changes the beam waist within the crystal, with a corresponding modification of the nonlinear conversion efficiency E_{NL} and with a concomitant reduction in mode-matching efficiency of the incident beam P_1 into the cavity. In order to obtain an estimate of the size and sign of these effects, we can calculate the temperature profile in our crystal by solving the heat diffusion equation with a source term given by the Gaussian profile of the cavity mode. Since the crystal has transverse dimensions 3 mm × 3 mm that are much larger than the fundamental beam waist $w_0 \simeq 20$ μm, we model the crystal as a circular cylinder of radius $a = 1.5$ mm and then derive the temperature distribution in a straightforward fashion.[13] If we restrict our attention to radial coordinates $r \ll a$, we find the following parabolic approximation for the temperature difference $\Delta T(r)$ between the temperature at a radial position r and that at the edge of the crystal:

$$\Delta T(r) = \Delta T(0)(1 - \alpha r^2),$$
$$\alpha \equiv \frac{2}{w_0^2}\left[\ln\frac{2\gamma a^2}{w_0^2} - Ei\left(-\frac{2a^2}{w_0^2}\right)\right]^{-1}, \quad (3)$$

with $\Delta T(0)$ estimated from the observed shift in the phase-matching temperature.[14] In Eq. (3), $Ei(x)$ is an exponential integral[15] and $\gamma \equiv 1.781$. Note that by referencing our result to the empirical value $\Delta T(0)$, we eliminate the need to deal in absolute

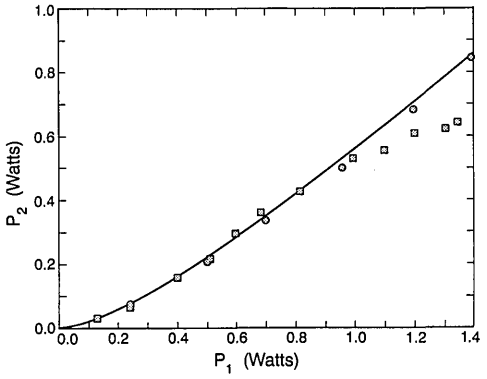

Fig. 2. Second-harmonic output power P_2 at 430 nm versus input fundamental power P_1 at 860 nm. The solid curve is the theoretical prediction based on the independently measured single-pass conversion efficiency and intracavity losses. The experimental points labeled by the squares are for cw operation with the external buildup cavity actively locked to the infrared input. The circles are obtained in a swept mode of operation to avoid thermal effects, with P_2 the peak power. In each case P_2 is referenced to the power level just outside the crystal face. Propagation losses to detector D_2 are (20 ± 5)%.

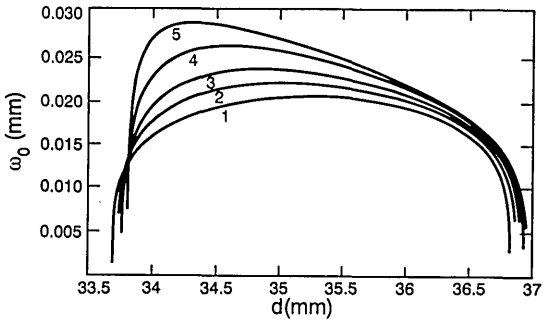

Fig. 3. Fundamental waist size ω_0 versus the spacing d between the lenses and the crystal surfaces to investigate the role of thermal lensing. Curves 1–5 are for increasing values of the axial temperature difference of $\Delta T(0) = 0$, 0.6, 1.0, 1.4, and 1.6 K, respectively.

terms with the rate of heat disposition, thermal conductivity, etc.

The temperature gradient of Eq. (3) results in a variation of the index of refraction $n(r)$, which to the lowest order is given by

$$n(r) = n_0 + \frac{\partial n_b}{\partial T}\Delta T(r) \equiv n_0' + \frac{1}{2}n_2 r^2, \qquad (4)$$

where $n_2 \equiv -2\alpha\partial n_b/\partial T$. Our measured value of the temperature derivative for the b axis of $KNbO_3$ is $\partial n_b/\partial T = -5 \times 10^{-5}/\mathrm{K}$. Thus in the approximation of a parabolic temperature distribution, the crystal is taken to be a medium with a quadratic index profile, and the Gaussian beam parameters of the cavity then follow in a standard fashion.[16] In Fig. 3 we examine the dependence of the fundamental beam waist ω_0 in the center of the crystal on the spacing d (Fig. 1) for increasing values of $\Delta T(0)$. Note that in order to maintain a given waist in the presence of heating, d must be changed, with Fig. 3 indicating two regions where thermal effects are reduced near the edges of the stability range. A major approximation in our calculation for Fig. 3 is an assumption of a fixed waist in the crystal for the solution of Eq. (3). In fact, $\Delta T(r)$ modifies $n(r)$, which in turn changes ω_0 and hence $\Delta T(r)$. However, our self-consistent numerical solutions to this problem assuming constant $\Delta T(0)$ are quite similar to the curves shown in Fig. 3 for small $\Delta T(0) < 2$ K. For instance for $\Delta T(0) = 2$ K, the self-consistent solution is close to curve 4 in Fig. 3.

In the absence of compensation, the changes in waist size shown in Fig. 3 will have a deleterious effect on the doubling efficiency. For example, if the spacing d is fixed at $d = 34.5$ mm, we estimate from Fig. 3 that the effects of thermal lensing should begin to become pronounced for $\Delta T(0) \simeq$ 1–1.5 K, which corresponds to $P_1 \simeq 0.5$ W. For a higher value of $P_1 = 1.0$ W, we estimate from our self-consistent solution a reduction in E_{NL} of ~40% and a degradation in mode-matching efficiency of ~10%, which leads to an overall drop in doubling efficiency of ~45%. Both these estimates agree reasonably well with experimental results that we have obtained with fixed $d \sim$ 34.5 mm. On the other hand, our best experimental results are obtained by decreasing d to the left-hand region of Fig. 3 near $d = 33.8$ mm, where we find empirically from Fig. 2 much smaller reductions in efficiency, which indicates effective compensation up to $P_1 \simeq 1.0$ W. However, as shown in Fig. 2, the ability to compensate thermal effects by varying d degrades for $P_1 \geq 1.0$ W; operation near the left-hand edge of stability in Fig. 3 becomes too precarious for large $\Delta T(0)$.

In summary, we have reported an investigation of frequency doubling with $KNbO_3$ in an external resonator driven by the light from a single-frequency $Ti:Al_2O_3$ laser. An output of 0.65 W of cw blue light at 430 nm has been generated from 1.35 W of infrared input. The effects of thermal lensing have been studied as likely candidates for the observed reduction in cw efficiency evidenced in Fig. 2. Beyond these initial results, we have recently improved the intracavity passive losses to a level of 0.8% in a new doubling cavity and have obtained 60 mW of cw blue light for 100 mW of IR input.

We gratefully acknowledge the contributions of S. J. Gu to the early phases of this research and the cooperation of G. Mizelle of Virgo Optics. This research was supported by the U.S. Office of Naval Research, by the National Science Foundation, and by Venture Research International.

References

1. J. C. Bammert, J. Hoffnagle, and P. Günter, Appl. Opt. **24,** 1299 (1985).
2. T. Baer, M. S. Keirstead, and D. F. Welch, in *Digest of Conference on Lasers and Electro-Optics* (Optical Society of America, Washington, D.C., 1989), paper ThM5.
3. T. Baer, Spectra-Physics, Mountain View, Calif. (personal communication).
4. G. J. Dixon, C. E. Tanner, and C. E. Wieman, Opt. Lett. **14,** 731 (1989).
5. A. Hemmerich, D. H. McIntyre, C. Zimmermann, and T. W. Hänsch, Opt. Lett. **15,** 372 (1990).
6. W. J. Kozlovsky, W. Lenth, E. E. Latta, A. Moser, and G. L. Bona, Appl. Phys. Lett. **56,** 2291 (1990).
7. M. K. Chun, L. Goldberg, I. N. Duling III, and T. F. Carruthers, in *Digest of Conference on Lasers and Electro-Optics* (Optical Society of America, Washington, D.C., 1990), paper CWE2.
8. C. S. Adams and A. I. Ferguson, Opt. Commun. **79,** 219 (1990).
9. Crystals fabricated by G. Mizelle, Virgo Optics, Port Richey, Fla.
10. A. Ashkin, G. D. Boyd, and T. M. Dziedzic, IEEE J. Quantum Electron. **QE-2,** 109 (1966).
11. W. J. Kozlovsky, C. D. Nabors, and R. L. Byer, Opt. Lett. **12,** 1014 (1987).
12. R. W. P. Drever, J. L. Hall, F. V. Kowalski, T. Hough, G. M. Ford, A. G. Munley, and H. Ward, Appl. Phys. **B 31,** 97 (1983).
13. J. P. Gordon, R. C. C. Leite, R. S. Moore, S. P. S. Porto, and J. R. Whinnery, J. Appl. Phys. **36,** 3 (1965).
14. In fact the harmonic heat source has a waist $\sqrt{2}$ smaller than the fundamental waist ω_0, but we neglect this difference in our model.
15. E. Tahnke and F. Emde, *Tables of Functions* (Teubner, Berlin, 1938).
16. A. Yariv, *Quantum Electronics,* 3rd ed. (Wiley, New York, 1989).